Original Research Article

Chemoinformatic Design of Phthalazinone Analogues as Novel Dengue Virus NS2B-NS3 Protease Inhibitors with Enhanced Pharmacokinetics

Samuel Ndaghiya Adawara[1]* (iD), **Gideon Shallangwa Adamu[2]** (iD), **Paul Andrew Mamza[2], Ibrahim Abdulkadir [2]**

[1] Department of Pure and Applied Chemistry, Faculty of Science, University of Maiduguri, P.M.B. 1069, Maiduguri, Borno State, Nigeria

[2] Department of Chemistry, Faculty of Physical Sciences, Ahmadu Bello University, P.M.B. 1044, Zaria, Kaduna State, Nigeria

A R T I C L E   I N F O

A B S T R A C T

Dengue fever is the most common and important arthropod-borne viral illness in humans. However, no effective medications or vaccinations exist to prevent this condition. The dengue viral (DENV) protease non-structural protein (NS) 2B-3 is a possible target for antiviral treatment. Based on the lead compound reported in our earlier study, eight phthalazinone analogues were designed using a structure-based drug design approach, which involved systematic alterations to the various positions of the benzyl ring bearing carbamate pharmacophore and carbamate terminal chain length of the lead. These compounds were also evaluated for *in silico* ADME properties and drug-likeness. The molecular docking scores of the design ligands were greater than the template's binding score, ranging from -8.9 to -9.60 kcal/mol, and also higher than those of the Ribavirin and the co-crystalized protease ligand, which were -8.90, -6.10, and -8.10 kcal/mol, respectively. All of the developed ligands satisfied Lipinski's requirements with good synthetic accessibility (3.07–3.41) and a better ADME profile than the template, indicating that they were highly bioavailable and simple to synthesize in the laboratory. Phthalazinone derivatives with higher binding scores (-9.0 to -9.60 kcal/mol) were designed and found to interact well with the DENV NS2B-NS3 protease. The compounds also have significantly improved pharmacokinetic and ADME properties compared to their parent template. The designed compounds could be used as a starting point for developing potent DENV NS2B-NS3 protease inhibitors with suitable pharmacokinetic and ADME properties.

*Corresponding author: Adawara, Samuel Ndaghiya

✉ E-mail: agapalawa3@gmail.com

G R A P H I C A L   A B S T R A C T
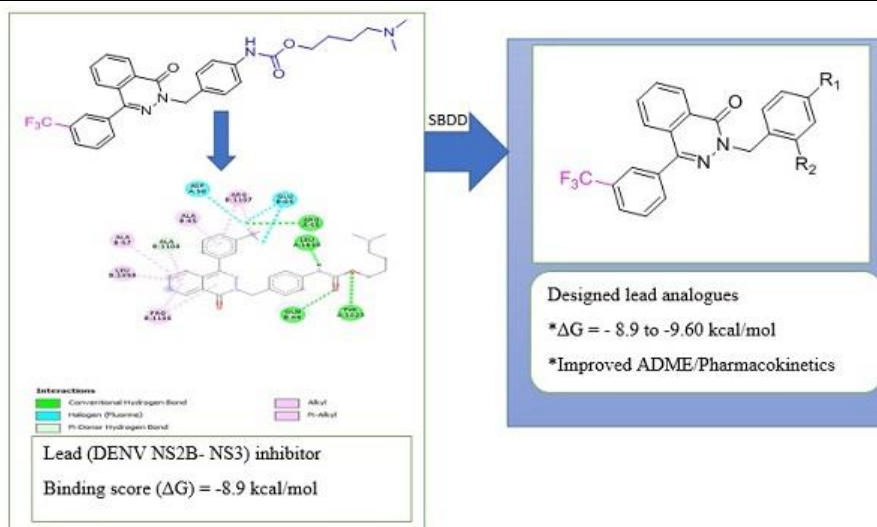
Introduction

An RNA arbovirus causes dengue fever; a Flavivirus carried by female mosquitoes (*Aedes* species), spread to many parts of the world at an epidemic rate, particularly in tropical and sub-tropical countries, posing a severe threat to the world's population in recent years [1]. DENV infection, if left untreated, can cause mild flu-like symptoms to more hemorrhagic severe fever or shock syndrome, which can lead to death [2, 3, 4].

The known four serotypes of DENV are DENV-1-4, with each having seven non-structural proteins (NS-1, NS-2A, NS-2B, NS-3, NS-4A, NS-4B, and NS-5) [4]. The NS3 protein, which creates the termini of numerous non-structural proteins, is the second-largest viral proteinase. NS2B is a cofactor for the NS3 viral serine protease activity, which is essential for Flavivirus polyprotein [5]. Each serotype can cause the disease independently of infection caused by another serotype, which should have provided immunity against further infection. This has been attributed to antibody-dependent disease enhancement [6].

The dengue virus's NS3-NS2B protease, NS4B helicase, E protein, methyltransferase (MTase), and RNA-dependent RNA polymerase (RdRp) have all recently been identified as potential antiviral therapeutic targets [7–10]. Dengue virus proteases are stable and evolutionarily conserved across serotypes. An N-terminal serine protease domain in DENV NS3 protease requires NS2B to be an active enzyme upon their complexation; NS3-NS2B. According to research, the protease can adopt a "closed" or "open" conformation. In the catalytically active closed state, NS2B is entirely bound to NS3 and becomes a component of the active site. NS2B is partially coupled to NS3 and far from the open and inactive conformation [11].

The rising prevalence of DENV infection, as well as the harmful health consequences for children and previously infected people, as well as the lack of approved treatments, necessitates immediate attention to the development of a more potent therapeutic agent to combat the disease's epidemic.

The traditional drug development method was costly, time-consuming, and complicated [12]. Drug research and discovery techniques such as structure-based approaches have become more cost-effective, timely, and efficient as computing

technology has advanced and many computational chemistry tools have been available [13, 14].

Knehans *et al.* (2011) used an in silico fragment-based drug design technique to find small molecule inhibitors of the DENV NS2B-NS3 protease. Compared to traditional high-throughput docking, this technique was thought to take less time. Only a small number of compounds must be docked, rather than millions [15]. Many *in silico* methodologies for predicting pharmacokinetic and toxicological features of drugs from their chemical structure have been developed [16].

Due to its success in the identification of lead compounds as well as the screening of vast compound databases for potentially active compounds [17, 18], molecular docking is becoming an impressively reliable structure-based approach among the structure-based approaches. Molecular docking studies are essential methodologies in structure-based drug design [17-18]. Molecular docking simulation can be used to predict the binding position of a protease and determine drug binding affinities on protease structures [19].

From high-throughput screening to an assessment of drug-likeness, bioavailability, and medicinal chemistry, the involvement of computer-aided drug development methodologies spanned the gamut. The ADME (Absorption, Distribution, Metabolism, and Excretion) features a large variety of biochemical compounds with a high potential for being active and meeting the requirements for promising therapeutics have been obtained using an *in silico* approach [20].

In this study, a lead derivative of phthalazinone discovered in a previous study was used in structure-based drug design [6]. Improved derivatives of the phthalazinone were then designed for viral protease inhibition based on the data and structural information from the lead's protein-ligand interaction.

These compounds have improved binding interactions and ADME features and can be developed as DENV NS3-NS2B protease inhibitors.

Materials and Methods

Lead compound and design

The data used in this investigation are the lead compounds identified in our prior work [6], as shown in Figure 1, in which we employed virtual screening to identify possible leads. This research was initiated to support a study in which compound 21 was identified as a potential lead. The active site amino acid residues of DENV-2 NS-5 protease docked favorably with compound 21, which had an excellent docking score of – 8.9 10 kcal/mol [6].
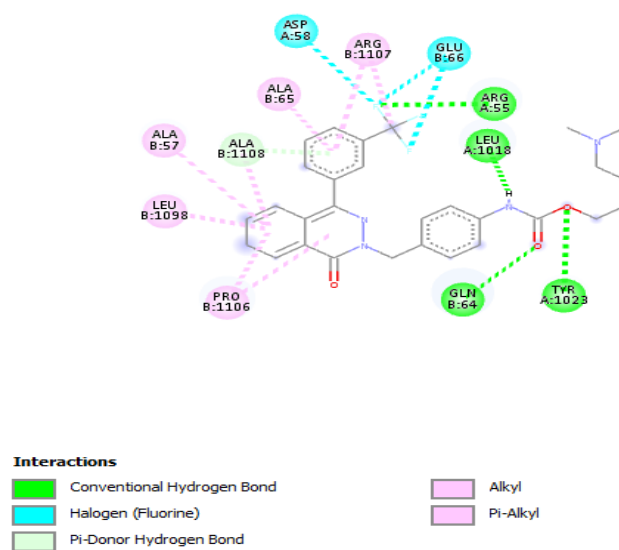
Figure 1. 2-D interaction type between ligand 21 and the target [6]

The analogs of the lead compound were designed by substituting, adding, or removing side-chain atoms in the structure of the selected lead compound [6, 11]. The design involved:
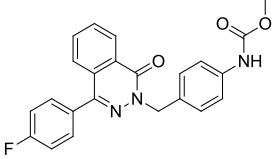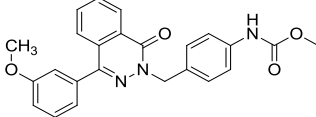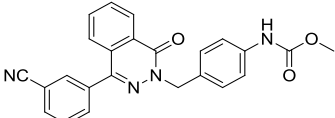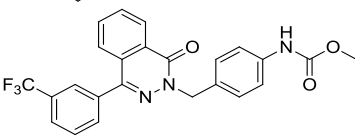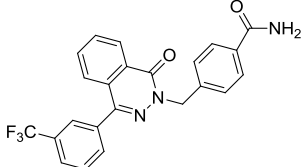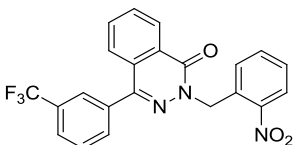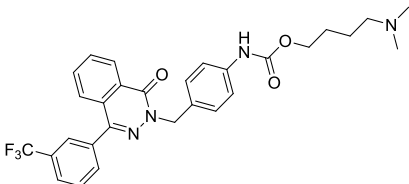
(i) Removal of the dimethylamino)butyl of the carbamate;

(ii) Substitution of the carbamate at para by amide, 1, 2, 4, oxadiazole, 1, 3, 4, oxadiazole,

and nitro-group (-NO$_2$) groups at the para position of the phenyl pharmacophore.

With that, a systematic substitution on the lead's' A phenyl pharmacophore produced lead analogs with carbamate terminal alterations. A total of eight lead analogs were designed for this purpose.

The different lead analogs with phthalazinone core were the generated ligand molecules. The 2-dimensional chemical structures (2D) of the compounds were drawn using the Chemdraw software [21] (Table 1).

Table 1. 2D Structures of the designed phthalazinone derivatives from the lead

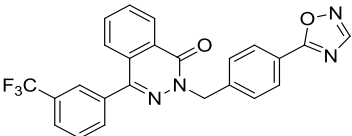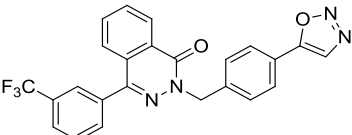| ID	Structure	IUPAC Name
2a		methyl (4-((4-(4-fluorophenyl)-1-oxophthalazin-2(1H)-yl)methyl)phenyl)carbamate
19a		methyl (4-((4-(3-methoxyphenyl)-1-oxophthalazin-2(1H)-yl)methyl)phenyl)carbamate
20a		methyl (4-((4-(3-cyanophenyl)-1-oxophthalazin-2(1H)-yl)methyl)phenyl)carbamate
21a		methyl (4-((1-oxo-4-(3-(trifluoromethyl)phenyl)phthalazin-2(1H)-yl)methyl)phenyl)carbamate
21b		4-((1-oxo-4-(3-(trifluoromethyl)phenyl)phthalazin-2(1H)-yl)methyl)benzamide
21c		2-(4-(1,2,4-oxadiazol-5-yl)benzyl)-4-(3-(trifluoromethyl)phenyl)phthalazin-1(2H)-one
21d		2-(4-(1,2,3-oxadiazol-5-yl)benzyl)-4-(3-(trifluoromethyl)phenyl)phthalazin-1(2H)-one
21e		2-(2-nitrobenzyl)-4-(3-(trifluoromethyl)phenyl)phthalazin-1(2H)-one
21 Template [6, 11]		4-(dimethylamino)butyl (4-((1-oxo-4-(3-(trifluoromethyl)phenyl)phthalazin-2(1H)-yl)methyl)phenyl)carbamate

Pre-docking preparation

Spartan 14 was used to convert the 2D chemical structure of a substance into 3D structures, which were then optimized. We used energy minimization to determine the optimal conformation for the hypothetical compounds after drawing their chemical structures and converting them to a PDB-readable file format. The energy minimization was performed utilizing the B_3LYP (Lee-Yang-Parr hybrid functional) level of the Density Function Theory technique implemented in Spartan 14 using 6-31G* as the basis set [22, 23].

The DENV protease, which was previously employed as a target in our prior work, was used in this study and obtained from the Protein Data Bank at http://www.rcsb.org/pdb (PDB ID: 6MO1). The protease was acquired in a complex with another compound (potential target inhibitor) [24]. As described [6], the protease was refined by removing heteroatoms and water molecules and adding hydrogen for a docking simulation.

Docking calculation/virtual screening

Autodock vina PyRx, a computational drug discovery software used for screening libraries of compounds against possible drug targets [25], was used to dock the protease (PDB ID: 6MO1) and the proposed compounds to determine their binding mode/affinity. Before docking calculations, the protease was prepared in Discovery Studio 2017, and the binding interaction mode was visualized [26].

Ribavirin was also considered a reference inhibitor based on our prior study. It was regarded as the standard inhibitor due to the lack of a licensed drug to treat dengue virus infection.

To back up our findings, the co-crystal ligand acquired in association with the protease from the PDB was isolated, optimized, and re-docked with the protease.

The docking scores and their poses were taken for further study. After docking, the ligands were ranked according to their binding energy. Post docking analysis was carried out using Discovery Studio to visually inspect the interactions to better understand the binding site residues involved and the mode of interaction (ligand-protease complex).

The designed inhibitors' ADME

The Swiss-ADME online program was used to determine the drug-likeness and pharmacokinetic features of the designed phthalazinone derivatives. Despite having favorable docking contact with the therapeutic target, the ADME evaluation of the designed molecule is critical in identifying potential failures in terms of drug-likeness and pharmacokinetics of the phthalazinone derivatives as potential drug candidates [27].

Results

The molecular docking results for the designed compounds

The proposed compounds' 2D chemical structures, and the template lead compound, are provided in Table 1. The proposed compounds differ from the template in the carbamate terminal length, the substitution of 1, 2, 3 and 1, 3, 4-oxaxadizole at the para position of the phenyl containing the carbamate, and the nitro-group on the meta-position of the phenyl bearing the carbamate.

Table 2 reveals the results of the docking binding affinity score (kcal/mol) of the designed compounds along with interaction information on the nature, kinds, and interaction bond lengths obtained using the Discovery studio after docking with protease using the vina-PyRx software. The scores ranged from -8.9 to -9.60 kcal/mol, implying that they were better than the lead.

Figures 2a–2j illustrate the 2D visual inspection results of the interaction between the designed ligand and the protease generated by the Discovery studio. The absence of unstable and unfavorable interactions indicated that the ligand-complexes had favorable interactions [28-29].

Designed compounds predicted ADME/Pharmacokinetics

Table 3 shows the findings of the proposed compounds' expected drug-likeness, pharmacokinetics, and ADME characteristics. Lipinski's recommendations for drug-likeness and oral bioavailability, gastrointestinal adsorption, PAINS alert synthetic accessibility, and bioavailability score are shown in Table 3.

Discussion

Molecular docking of the designed compounds with the target

The molecular docking results of the designed phthalazinone analogs (Table 1) are presented in Table 2. The docking scores of the phthalazinone analogues (2a, 19a,20a, 21a, 21b, 21c, 21d, and 21e) discovered in this work (Table 2) were -9.00, -8.90, 9.00, 9.30, -9.30,-9.60,-9.40, and -9.20 kcal/mol, respectively, while the lead had a docking value of -8.90 kcal/mol [6]. Compounds 2a, 19a, and 20a are analogs of compounds 2, 19, and 20 [6], also had a better docking score. Compound 19a had a similar docking score to the lead compound but was chosen because of its favorable predicted pharmacokinetics profile compared to the lead. In contrast, compounds 2a and 20a had a better binding score than the lead. Aside from having improved binding scores, their existence in this work illustrates the viability of Meta position and para position of the phenyl ring, having the $-CF_3$, $-OCH_3$, and $-CN$ groups in each case correspondingly.

Compounds 21a, 21b, 21c, 21d, and 21e are lead analogs with substantially higher binding scores

than lead (-9.20 to -9.60 kcal/mol), demonstrating the lead compounds' potential as parent compounds for designing more potent analogs. Interestingly, the proposed compounds outperformed both the referred inhibitor (ribavirin) and the co-crystallized protease ligand with binding scores of -6.10 and -8.10 kcal/mol, respectively, in addition to outperforming the lead (Table 2).

Compound 2a was found to form two primary conventional hydrogen bonds with the ARG-55 and GLU-66 (2.153 and 2.345 Å) residues. Two carbon-hydrogen bonds involving fluorine with ALA-65 and LEU-53 residues were observed, respectively. Furthermore, two halogens and two Pi-Donor Hydrogen Bond interactions were formed with GLN-64, ALA-1108, GLN-64, and ALA-1108 residues. In contrast, the remaining eight interactions were all Hydrophobic (Hydp) (ALA-57, LEU-1098, PRO-1106, ALA-1108, ARG-55, ALA-65, ARG-1107, ALA-1108) through alkyl and Pi-alkyl and Pi-alkyl groups (Figure 2a and Table 2).

Compound 19a with a binding score precisely as the lead could be seen to form only one conventional hydrogen bond (2.11 Å) with ARG55 residue, while two residues of the protease interacted through (LEU-53 and ASP-58) the carbon-hydrogen bond and the other two (GLN-64 and ALA-1108) through the pi-donor hydrogen bond. The dominant interaction involves Hpb involving ALA-57, LEU-1098, PRO-1106, ALA-1108, ARG-55, ALA-65, ARG-1107, and ALA-1108 through Alkyl and Pi-Alkyl (Figure 2b and Table 2).

ARG-55 (2.11 Å) residue formed the essential conventional hydrogen bond in compound 20a, with a binding score of -9.0 kcal/mol. In contrast, the other three hydrogen bonds (LEU-53, GLN-64, and ALA-1108) occurred via carbon-hydrogen bond, pi-donor hydrogen bond, and pi-donor hydrogen bond interactions, respectively. Hpb interactions with ALA-57, LEU-1098, PRO-1106, ALA-1108, ALA-65, ARG-1107, and ALA-

1108 residues were mainly formed via Alky and Pi-Alkyl (Figure 2c and Table 2).

Compounds 21a to 21d, the lead analogs, had a much better binding affinity (-9.20 to 9.60 kcal/mol) (Table 2). In compound 21a, with a docking score of -9.30 kcal/mol, ARG-55, ARG-55, ARG-55, GLN-64 (2.127, 2.54, 2.53, and 2.89 Å), amino acid residues of the protease formed conventional hydrogen bond interactions with it. Among the conventional hydrogen bonds formed in these interactions, fluorine was observed to be involved (ARG-55 and GLN-64) (Figure 2d and Table 2). The other three hydrogen bonds observed in compound 21a (Figure 2d and Table 2) involved LEU-53, GLN-64, and ALA-1108 through Carbon Hydrogen Bond, Pi-Donor Hydrogen Bond, and Pi-Donor Hydrogen Bond, respectively. Five halogen-related interactions have been associated with ASP-58, ASP-58, ASP-58, GLU-66, and GLU66 residues (Table 2). The Hpb region residues involved were ALA-57, LEU-1098, PRO-1106, ALA-1108, ARG-1107, ARG-55, ALA-65, and ALA-1108.

Despite having the same docking score (-9.30 kcal/mol) as compound 21a, compound 21b appears to have fewer contacts than compound 21a. This could be due to the presence of fluorine, which has been shown to help stabilize interactions. ARG-55 and ASN1105 (2.873 and 2.05 Å) interacted with the fluorine of compound 21b (Figure 2e) in the conventional hydrogen bond interactions that stabilized it, whereas PRO-1106, ARG-1107, and other residues were seen to interact with the fluorine of compound 21b. There was also one electrostatic interaction (GLU-62) involving ALA-65, ALA-1108, ALA-1108, LEU-1098, PRO-1106, ARG-1107, and ARG-1107 account for the seven Hypb interactions via Alkyl and Pi-Alkyl.

Among the designed phthalazinone derivatives, compound 21c has the best binding affinity (-9.60 kcal/mol) to the protease (Table 2). In addition to the presence of fluorine, which is known to stabilize the complex [25], the substitution of the carbamate moiety of the lead with the 1, 2, 4-oxadiazole moiety could account for the improvement in the binding score. The amino acid residues GL-N64 and LEU-53 (2.446 and 2.797) were found to form conventional hydrogen bonds (Figure 2f). At the same time, four halogen interactions involving fluorine were discovered (GLU-66, GLU-66, and ALA-1108), and one hydrogen bond via the Pi-Donor Hydrogen Bond was discovered involving the ALA-1108 residue. The other interactions with ALA-57, PRO-1106, ARG-1107, ARG-55, ALA-65, and ALA-1108 are accounted for by six Hypb interactions via alkyl and pi-alkyl.

Compound 21d is very close to compound 21c and has the second-highest binding score (-9.40 kcal/mol). The importance of the oxadiazole moiety in increasing the activity of this class of molecule is highlighted by this. In compound 21d, only one typical hydrogen bond was established, linking one nitrogen of the phthalazin core with GLN-64 (2.573 Å), as shown in Table 2 and Figure 2g. In contrast, the four halogen contacts involved three GLU-66 and one ALA1108 amino acid residue (Figure 2g and Table 2). Furthermore, the ALA-1108 residue was revealed to be involved in the single hydrogen bond detected using the Pi-Donor Hydrogen Bond, while the eight residues that constitute the Hypb are TYR-1023, ALA-57, PRO-1106, ARG-1107, ARG-55, ARG-55, ALA-65, and ALA-1108.

Three conventional hydrogen bonds with ARG-55, GLN-64, and GLN-64 (2.853, 2.267, and 2.738 Å) residues were observed in compound 21e, which had a binding score of -9.40 kcal/mol (Table 2), and one fluorine was also involved. In contrast, the other two halogen interactions involved ASP-58 and GLU-66 amino acid residues of the protease. The Pi-anion formed an electrostatic contact with the GLU-62 residue. The other two hydrogen interactions in compound 21e were with the protease's GLN-64 and ALA-1108 residues via a Pi-Donor Hydrogen

Bond. In contrast, nine Hypb contacts were found (ALA-57, LEU-1098, PRO-1106, ALA-1108, ARG-1107, ALA-65, ARG-1107, ALA-1108, and ARG-55), mainly on the Phthalazinone core (Figure 2h).

Table 2. Detailed illustration of the bonding interaction terms between the designed ligands and the protease

Inhibitor- protease complex Binding affinity (kcal/mol)	Amino acid residue	Distance (Å)	Category	Types
	A:ARG55	2.15313	Hydrogen Bond	Conventional Hydrogen Bond
	B:GLU66	2.34596	Hydrogen Bond; Halogen	Conventional Hydrogen Bond; Halogen (Fluorine)
	B:ALA65	3.17975	Hydrogen Bond; Halogen	Carbon Hydrogen Bond; Halogen (Fluorine)
	A:LEU53	3.66225		
	B:GLN64	3.56933	Hydrogen Bond	Carbon Hydrogen Bond
	B:ALA1108	3.17809	Halogen	Halogen (Fluorine)
	B:GLN64	3.04968	Halogen	Halogen (Fluorine)
2a-6MO1	B:ALA1108	2.68973	Hydrogen Bond	Pi-Donor Hydrogen Bond
-9.0	B:ALA57	4.76787	Hydrogen Bond	Pi-Donor Hydrogen Bond
	B:LEU1098	5.126	Hydp	Alkyl
	B:PRO1106	4.54624	Hydp	Alkyl
	B:ALA1108	5.00406	Hydp	Alkyl
	A:ARG55	5.32881	Hydp	Alkyl
	B:ALA65	5.40494	Hydp	Pi-Alkyl
	B:ARG1107	4.78505	Hydp	Pi-Alkyl
	B:ALA1108	4.58038	Hydp	Pi-Alkyl
			Hydp	Pi-Alkyl
	A:ARG55	2.11839	Hydrogen Bond	Conventional Hydrogen Bond
	A:LEU53	3.79914	Hydrogen Bond	Carbon Hydrogen Bond
	A:ASP58	3.35837	Hydrogen Bond	Carbon Hydrogen Bond
	B:GLN64	3.06777	Hydrogen Bond	Pi-Donor Hydrogen Bond
	B:ALA1108	2.75136	Hydrogen Bond	Pi-Donor Hydrogen Bond
19a-6MO1	B:ALA57	4.7748	Hydp	Alkyl
-8.9	B:LEU1098	5.11351	Hydp	Alkyl
	B:PRO1106	4.55495	Hydp	Alkyl
	B:ALA1108	4.98925	Hydp	Alkyl
	A:ARG55	5.35972	Hydp	Pi-Alkyl
	B:ALA65	5.24778	Hydp	Pi-Alkyl
	B:ARG1107	5.03639	Hydp	Pi-Alkyl
	B:ALA1108	4.49057	Hydp	Pi-Alkyl
	A:ARG55	2.11588	Hydrogen Bond	Conventional Hydrogen Bond
	A:LEU53	3.74653	Hydrogen Bond	Carbon Hydrogen Bond
	B:GLN64	3.06112	Hydrogen Bond	Pi-Donor Hydrogen Bond
	B:ALA1108	2.77225	Hydrogen Bond	Pi-Donor Hydrogen Bond
20a-6MO1	B:ALA57	4.73972	Hydp	Alkyl
-9.0	B:LEU1098	4.95832	Hydp	Alkyl
	B:PRO1106	4.76559	Hydp	Alkyl
	B:ALA1108	4.92044	Hydp	Alkyl
	B:ALA65	5.40242	Hydp	Pi-Alkyl
	B:ARG1107	5.03344	Hydp	Pi-Alkyl
	B:ALA1108	4.5464	Hydp	Pi-Alkyl

Table 2. Continued

Inhibitor- protease complex Binding affinity (kcal/mol)	Amino acid residue	Distance (Å)	Category	Types
	A:ARG55	2.12778	Hydrogen Bond	Conventional Hydrogen Bond
	A:ARG55	2.5488	Hydrogen Bond; Halogen	Conventional Hydrogen Bond; Halogen (Fluorine)
	A:ARG55	2.53654	Hydrogen Bond; Halogen	Conventional Hydrogen Bond; Halogen (Fluorine)
	B:GLN64	2.89732		
	A:LEU53	3.72082	Hydrogen Bond	Conventional Hydrogen Bond
	A:ASP58	3.08298	Hydrogen Bond	Carbon Hydrogen Bond
	A:ASP58	3.26497	Halogen	Halogen (Fluorine)
	A:ASP58	3.68665	Halogen	Halogen (Fluorine)
	B:GLU66	3.38568	Halogen	Halogen (Fluorine)
21a-6MO1	B:GLU66	2.81477	Halogen	Halogen (Fluorine)
-9.30	B:GLN64	3.0427	Halogen	Halogen (Fluorine)
	B:ALA1108	2.89439	Hydrogen Bond	Pi-Donor Hydrogen Bond
	B:ALA57	4.79594	Hydrogen Bond	Pi-Donor Hydrogen Bond
	B:LEU1098	5.20248	Hydp	Alkyl
	B:PRO1106	4.53323	Hydp	Alkyl
	B:ALA1108	5.03239	Hydp	Alkyl
	B:ARG1107	4.57486	Hydp	Alkyl
	A:ARG55	5.28666	Hydp	Alkyl
	B:ALA65	5.16171	Hydp	Pi-Alkyl
	B:ALA1108	4.51595	Hydp	Pi-Alkyl
			Hydp	Pi-Alkyl
	A:ARG55	2.87397	Hydrogen Bond	Conventional Hydrogen Bond
	B:ASN1105	2.05199	Hydrogen Bond	Conventional Hydrogen Bond
	B:PRO1106	3.31299	Halogen	Halogen (Fluorine)
	B:ARG1107	3.28846	Halogen	Halogen (Fluorine)
	B:GLU62	4.42973	Electrostatic	Pi-Anion
21b-6MO1	B:ALA65	5.08926	Hydp	Alkyl
-9.30	B:ALA1108	5.15293	Hydp	Alkyl
	B:ALA1108	4.29019	Hydp	Alkyl
	B:LEU1098	4.14464	Hydp	Alkyl
	B:PRO1106	4.82558	Hydp	Alkyl
	B:ARG1107	4.97832	Hydp	Pi-Alkyl
	B:ARG1107	5.2626	Hydp	Pi-Alkyl
	B:GLN64	2.44636	Hydrogen Bond	Conventional Hydrogen Bond
	A:LEU53	2.79757	Hydrogen Bond	Conventional Hydrogen Bond
	B:GLU66	3.27586	Halogen	Halogen (Fluorine)
	B:GLU66	3.31155	Halogen	Halogen (Fluorine)
	B:GLU66	3.52792	Halogen	Halogen (Fluorine)
21c-6MO1	B:ALA1108	3.06534	Halogen	Halogen (Fluorine)
-9.60	B:ALA1108	2.97434	Hydrogen Bond	Pi-Donor Hydrogen Bond
	B:ALA57	4.78821	Hydp	Alkyl
	B:PRO1106	4.57582	Hydp	Alkyl
	B:ARG1107	3.97175	Hydp	Alkyl
	A:ARG55	4.86725	Hydp	Pi-Alkyl
	B:ALA65	5.43484	Hydp	Pi-Alkyl
	B:ALA1108	4.52043	Hydp	Pi-Alkyl

Table 2. Continued

Inhibitor- protease complex Binding affinity (kcal/mol)	Amino acid residue	Distance (Å)	Category	Types
	B:GLN64	2.5738	Hydrogen Bond	Conventional Hydrogen Bond
	B:GLU66	3.25303	Halogen	Halogen (Fluorine)
	B:GLU66	3.50483	Halogen	Halogen (Fluorine)
	B:GLU66	3.27971	Halogen	Halogen (Fluorine)
	B:ALA1108	2.99925	Halogen	Halogen (Fluorine)
	B:ALA1108	2.91525	Hydrogen Bond	Pi-Donor Hydrogen Bond
21d-6MO1	A:TYR1023	5.12535	Hydp	Pi-Pi T-shaped
-9.40	B:ALA57	4.68448	Hydp	Alkyl
	B:PRO1106	4.57358	Hydp	Alkyl
	B:ARG1107	3.95539	Hydp	Alkyl
	A:ARG55	4.9296	Hydp	Pi-Alkyl
	A:ARG55	4.67887	Hydp	Pi-Alkyl
	B:ALA65	5.28008	Hydp	Pi-Alkyl
	B:ALA1108	4.40526	Hydp	Pi-Alkyl
	A:ARG55	2.85366	Hydrogen Bond; Halogen	Conventional Hydrogen Bond; Halogen (Fluorine)
	B:GLN64	2.26773	Hydrogen Bond	Conventional Hydrogen Bond
	B:GLN64	2.7377	Hydrogen Bond	Conventional Hydrogen Bond
	A:ASP58	3.46835	Halogen	Halogen (Fluorine)
	B:GLU66	3.40118	Halogen	Halogen (Fluorine)
	B:GLU62	3.6057	Electrostatic	Pi-Anion
	B:GLN64	2.84998	Hydrogen Bond	Pi-Donor Hydrogen Bond
	B:ALA1108	2.93044	Hydrogen Bond	Pi-Donor Hydrogen Bond
21e-6MO1	B:ALA57	4.8409	Hydp	Alkyl
-9.20	B:LEU1098	4.92626	Hydp	Alkyl
	B:PRO1106	4.89868	Hydp	Alkyl
	B:ALA1108	4.81219	Hydp	Alkyl
	B:ARG1107	4.22086	Hydp	Alkyl
	B:ALA65	5.36361	Hydp	Pi-Alkyl
	B:ARG1107	5.25279	Hydp	Pi-Alkyl
	B:ALA1108	4.59818	Hydp	Pi-Alkyl
	A:ARG55	5.05532	Hydp	Pi-Alkyl
	A:TYR1023	2.2839	Hydrogen Bond	Conventional Hydrogen Bond
	A:ASP58	2.317	Hydrogen Bond	Conventional Hydrogen Bond
	B:ASP58	2.751	Hydrogen Bond	Conventional Hydrogen Bond
	B:GLU62	3.425	Hydrogen Bond	Carbon Hydrogen Bond
	B:GLU62	3.532	Electrostatic	Pi-Anion
	B:GLN64	3.246	Hydrogen Bond	Pi-Donor Hydrogen Bond
-8.10	B:ALA1108	2.593	Hydrogen Bond	Pi-Donor Hydrogen Bond
	B:ALA57	5.413	Hydp	Pi-Alkyl
	B:ALA1108	4.933	Hydp	Pi-Alkyl
	A:ARG55	4.004	Hydp	Pi-Alkyl
	B:ARG1107	5.030	Hydp	Pi-Alkyl
	B:ALA1108	4.371	Hydp	Pi-Alkyl
	B:LEU1085	2.1162	Hydrogen Bond	Conventional Hydrogen Bond
	B:GLY1087	2.72455	Hydrogen Bond	Conventional Hydrogen Bond
	B:GLU1088	2.11424	Hydrogen Bond	Conventional Hydrogen Bond
-6.10	B:GLU1086	2.69959	Hydrogen Bond	Conventional Hydrogen Bond
	B:GLY1087	2.15165	Hydrogen Bond	Conventional Hydrogen Bond
	B:ILE1165	2.63017	Hydrogen Bond	Conventional Hydrogen Bond

Hydp= Hydrophobic

Ribavirin, which was reported to have a docking score of -6.10 and considered the reference inhibitor, had six conventional hydrogen bonds involving LEU-085, GLY-1087, GLU-1088 GLU-1086, GLY-1087, and ILE-1165 protease residues [6]. Despite having a higher number of conventional hydrogen bonds, its docking score could be seen to be lower than the lead and much lower than those of the designed phthalazinone derivatives. This highlights the importance of various interaction types and the potential of the designed compounds as DENV inhibitors.
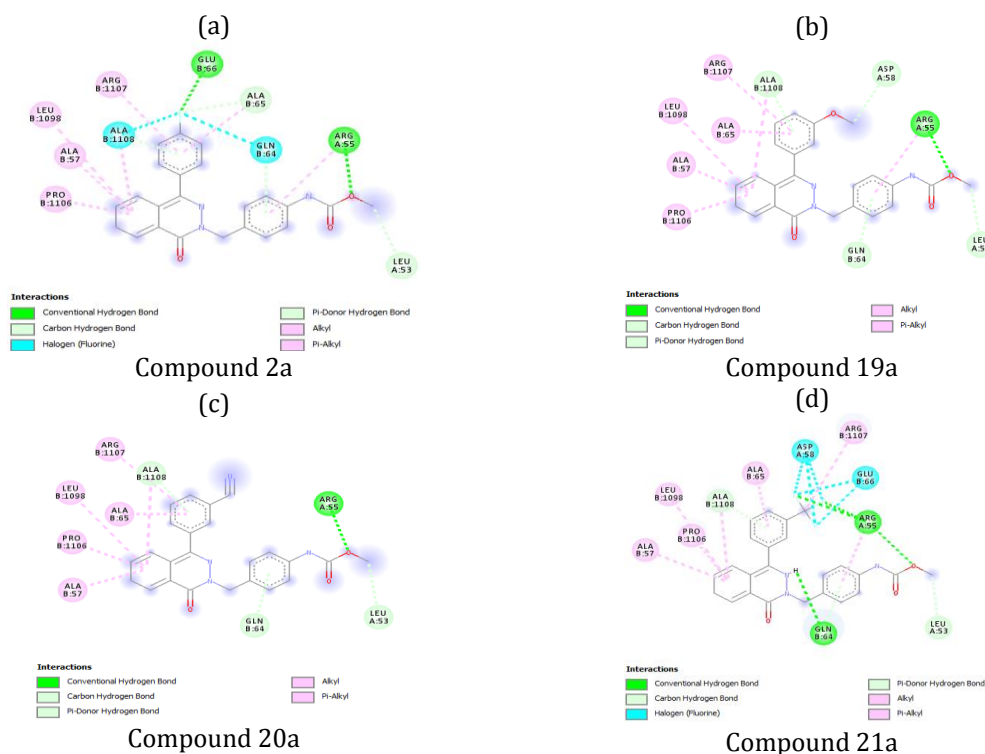
When the co-crystal ligand of the protease was re-docked (binding score of -8.10 kcal/mol) (Table 2) with the protease, three conventional hydrogen bonds could be observed with TYR-1023, ASP-58, and ASP-58 (2.2839, 2.317, and 2.751 Å), respectively. The two GLU-62 residues have been involved in hydrogen bonds and electrostatic interactions through carbon-hydrogen bonds and pi-anion (Figure 2-j). Hypb interactions are facilitated by the residues ALA-57, ALA-1108, ARG-55, ARG-1107, and ALA-1108. The co-crystal ligand of the protease's binding score is observed to be much lower than
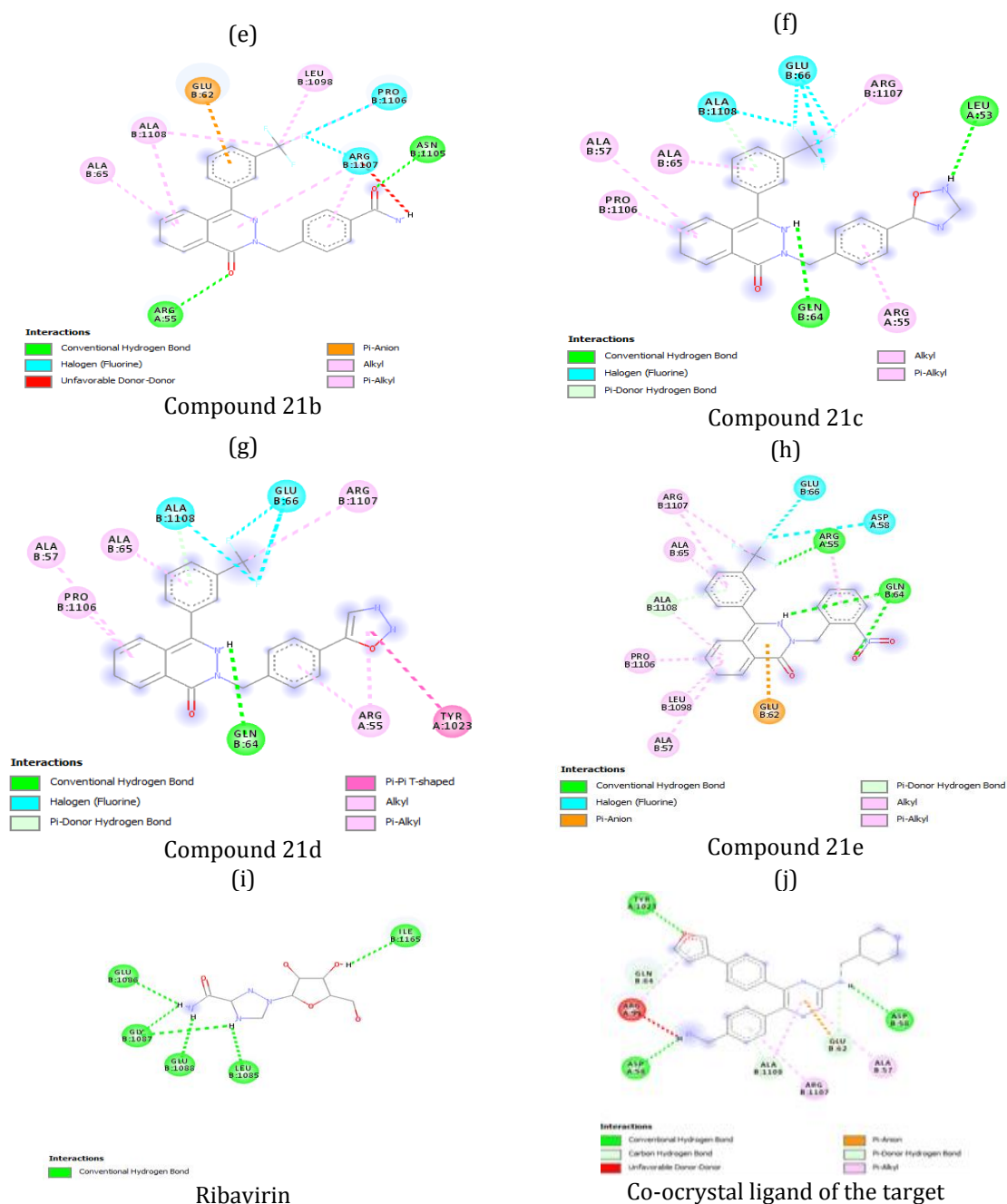
the lead as well, as the designed inhibitor could also be seen to possess unfavorable interaction, which decreases its stability. It was also observed to have some common amino acid residues with the designed compounds.

More importantly, in all of the proposed compounds, the presence of fluorine was seen to be stabilized by conventional hydrogen. This highlights the relevance of fluorine at meta and para positions in ensuring the stability of ligand protease complexes.

The compounds all had favorable interactions with the protease, indicating that they have a lot of potential as inhibitors. Among the developed compounds, compounds 21a-21e had a remarkable docking score that was significantly superior to the lead, referenced inhibitor, and co-crystallized ligand of the protease.

The designed compound-protease complexes were mostly stabilized by conventional hydrogen bond and Hydp bond interactions involving residues at the protease's allosteric locations, implying that they will interact with the protease more favorably than the template was found to work in the same way as conventional inhibitors.

(a)

Compound 2a

(b)

Compound 19a

(c)

Compound 20a

(d)

Compound 21a

(e)

Compound 21b

(f)

Compound 21c

(g)

Compound 21d

(h)

Compound 21e

(i)

Ribavirin

(j)

Co-ocrystal ligand of the target

Figure 2. The interaction of some selected design compounds and a conventional inhibitor (ribavirin) with the protease in two dimensions (PDB ID: 6MO1)

ADME of designed phthalazinone derivatives

The drug-likeness of every potential therapeutic candidate is crucial in the drug design process. The Swiss-ADME web application applied the drug-likeness, ADME, and PK characteristics for designed compounds proposed by Lipinski. The drug-likeness, ADME, and PK parameters that were obtained are listed in Table 3.

All of the designed compounds were found to follow Lipinski's rules, which included a molecular weight of at least 500, a log P value of at least 5, hydrogen-bond donors of at least 5, hydrogen-bond acceptors of at least 10, and a

topological polar surface area (TPSA) of at least 140 [30] [20]. In contrast, the lead violated 2 of the rules (Table 3). Estimating the ease of synthesis (synthetic-accessibility) of bioactive compounds possessing drug-likeness is an essential need in the drug discovery process [31]. The gastro-intestinal adsorption (GIA), pan-assay interference chemicals (PAINS) alert, bioavailability score, and synthetic accessibility are all valuable pieces of information derived from the ADME evaluation provided in Table 3. Except for lead with low GIA, all the designed ligands appeared to have a high GIA, implying that the designed ligands have a simple and favorable GIA. No PAINS warning was seen (Table 3) in any of the compounds, including the standard, which displays the genuine activity of the compounds in biochemical assays. The designed ligands were observed to have no PAINS alerts [32].

The designed compounds' bioavailability scores and the standards all fall into the active category, and compounds with bioavailability scores in this range are characterized as very active [33]. The compounds all displayed ease of synthesis, as proven by their synthetic accessibility scores of less than 4, lower than the norms. The lower the value, the easier a chemical compound may be synthesized [31].

Isoforms of enzymes' drug-metabolizing capacity, clinically significant CYP450 genetic variants, cytochrome P450 CYP-1A2, CYP-2C9, CYP-2C19, and CYP-2D6 were all assessed. Table 3 demonstrates that the proposed ligands are non-Pgp substrates, but the lead appears to be a Pgp substrate. Compounds 19a, 21b, 21c, and 21d were non-inhibitors of CYP-1A2, while all the compounds except for the lead appeared to be non-inhibitors CYP2D6. Except for compounds 19a and 20a, none of the designed ligandsis an inhibitor of CYP3A4 (Table 3) [34-35].

Table 3. ADME/pharmacokinetics parameters of the designed ligands

Molecule	2a	19a	20a	21a	21b	21c	21d	21e	Template (lead)
MW	403.41	415.44	410.42	453.41	423.39	448.4	448.4	425.36	538.56
#H-bond acceptors	5	5	5	7	6	8	8	7	8
#H-bond donors	1	1	1	1	1	0	0	0	1
TPSA	73.22	82.45	97.01	73.22	77.98	73.81	73.81	80.71	76.46
MLOGP	3.95	3.25	2.92	4.36	4.16	4.26	4.4	4.02	4.55
Consensus Log P	4.05	3.75	3.53	4.78	4.27	4.98	4.93	4.35	5.48
GI absorption	High	High	High	High	High	High	High	High	Low
Pgp substrate	No	No	No	No	No	No	No	No	Yes
CYP1A2 inhibitor	Yes	No	Yes	Yes	No	No	No	Yes	Yes
CYP2C19 inhibitor	Yes	Yes	Yes	Yes	Yes	Yes	Yes	Yes	Yes
CYP2C9 inhibitor	Yes	Yes	Yes	Yes	Yes	Yes	Yes	Yes	Yes
CYP2D6 inhibitor	No	No	No	No	No	No	No	No	Yes
CYP3A4 inhibitor	No	Yes	Yes	No	No	No	No	No	Yes
Lipinski #violations	0	0	0	1	1	1	1	0	2
Bioavailability Score	0.55	0.55	0.55	0.55	0.55	0.55	0.55	0.55	0.17
PAINS #alerts	0	0	0	0	0	0	0	0	0
Synthetic Accessibility	3.07	3.25	3.19	3.26	3.12	3.41	3.6	3.31	4.03

Conclusion

We designed 8 novel inhibitors of dengue virus NS3-NS2B protease based on systematic modifications to the various positions of the benzyl ring as well as the carbamate pharmacophore by oxadiazole, nitro-group, and reduction of the carbamate terminal chain to obtain derivatives of the lead with better inhibitory activity through molecular docking from the lead compound (21) from our previous work. The proposed ligands all outperformed the lead in terms of docking binding scores as well as pharmacokinetic profiles, demonstrating a higher binding affinity for the NS2B-NS3 binding pocket. The docking studies also revealed that compound 21c, with a binding score of -9.60 kcal/mol, is the most promising. The findings also demonstrated the importance of carbamate terminal length. The compounds discovered in this study could be synthesized as potential antiviral candidates against DENV due to their high binding affinity and favorable interactions with the DENV NS3-NS3 protease responsible for the replication of the virus, as well as better pharmacokinetics. The findings of this study could be extremely beneficial to the pharmaceutical sector in terms of obtaining potent DENV inhibitors at a low cost and in a timely manner, potentially lowering prices when compared to traditional, time-consuming, and costly approaches.

Acknowledgment

Disclosure statement

No potential conflict of interest was reported by the authors.

ORCID

Samuel N. Adawara : 0000-0002-8789-7871
Gideon S. Adamu : 0000-0002-0700-9898

References

[1] S. Bhatt, P.W. Gething, O.J. Brady, J.P. Messina, A.W. Farlow, C.L. Moyes, J.M. Drake, J.S. Brownstein, A.G. Hoen, O. Sankoh, M.F. Myers, *Nature*, **2013**, *496*, 504–507. [CrossRef], [Google Scholar], [Publisher]

[2] D. Megawati, S. Masyeni, B. Yohan, A. Lestarini, R.F. Hayati, F. Meutiawati, K. Suryana, T. Widarsa, D.G. Budiyasa, N. Budiyasa, K.S. Myint, *Plos negl. Trop. Dis.*, **2017**, *11*, e0005483. [CrossRef], [Google Scholar], [Publisher]

[3] N.A. Abdelkader, *Egypt. J. Intern. Med.*, **2018**, *30*, 47–48. [CrossRef], [Google Scholar], [Publisher]

[4] F. Batool, M. Saeed, H.N. Saleem, L. Kirschner, J. Bodem, *Pathogens*, **2021**, *10*, 464. [CrossRef], [Google Scholar], [Publisher]

[5] P. Parida, R.N. Yadav, K. Sarma, L. Mohan Nainwal, *Curr. Pharm. Biotechnol.*, **2013**, *14*, 995–1008. [Google Scholar], [Publisher]

[6] S.N. Adawara, G.A. Shallangwa, P.A. Mamza, A. Ibrahim, *Beni-Suef University Journal of Basic and Applied Sciences*, **2020**, *9*, 1–17. [CrossRef], [Google Scholar], [Publisher]

[7] C. Nitsche, S. Holloway, T. Schirmeister, C.D. Klein, *Chemical reviews*, **2014**, *114*, 11348–11381. [CrossRef], [Google Scholar], [Publisher]

[8] S.P. Lim, Q.Y. Wang, C.G. Noble, Y.L. Chen, H. Dong, B. Zou, F. Yokokawa, S. Nilar, P. Smith, D. Beer, J. Lescar, *Antivir. Res.*, **2013**, *100*, 500–519. [CrossRef], [Google Scholar], [Publisher]

[9] S.P. Lim, C.G. Noble, C.C. Seh, T.S. Soh, A. El Sahili, G.K. Chan, J. Lescar, R. Arora, T. Benson, S. Nilar, U. Manjunatha, *Plos Pathog.,* **2016**, *12*, e1005737. [CrossRef], [Google Scholar], [Publisher]

[10] J. Suganya, R. Mahendran, *Int. J. Pharm. Bio Sci.,* **2016**, *7*, 1135–1144. [CrossRef], [Google Scholar], [Publisher]

[11] D. Lu, J. Liu, Y. Zhang, F. Liu, L. Zeng, R. Peng, L. Yang, H. Ying, W. Tang, W. Chen, J.

Zuo, *Eur. J. Med. Chem.*, **2018**, *145*, 328–337. [CrossRef], [Google Scholar], [Publisher]

[12] T. Wang, M.B. Wu, J.P. Lin, L.R. Yang, *Expert Opin. Drug Discov.*, **2015**, *10*, 1283–1300. [CrossRef], [Google Scholar], [Publisher]

[13] S.J. Macalino, J.B. Billones, V.G. Organo, M.C. Carrillo, *Molecules*, **2020**, *25*, 665. [CrossRef], [Google Scholar], [Publisher]

[14] S. Anusuya, D. Velmurugan, M.M. Gromiha, *J. Biomol. Struct. Dyn.*, **2016**, *34*, 1512–1532. [CrossRef], [Google Scholar], [Publisher]

[15] T. Knehans, A. Schüller, D.N. Doan, K. Nacro, J. Hill, P. Güntert, M.S. Madhusudhan, T. Weil, S.G. Vasudevan, *J. Comput. Aided Mol. Des.*, **2011**, *25*, 263–274. [CrossRef], [Google Scholar], [Publisher]

[16] C. Shekhar, *Chem. Biol.*, **2008**, *15*, 413–414. [CrossRef], [Google Scholar], [Publisher]

[17] F. Benmansour, C. Eydoux, G. Querat, X. de Lamballerie, B. Canard, K. Alvarez, J.C. Guillemot, K. Barral, *Eur. J. Med. Chem.*, **2016**, *109*, 146–156. [CrossRef], [Google Scholar], [Publisher]

[18] M.T. ul Qamar, S. Kiran, U.A. Ashfaq, M.R. Javed, F. Anwar, M.A. Ali, A.H. Gilani, , *Int. J. Pharmacol.*, **2016**, *12*, 621–632. [CrossRef], [Google Scholar], [Publisher]

[19] X.Y. Meng, H.X. Zhang, M. Mezei, M. Cui, *Curr. Comput.-Aided Drug. Des.*, **2011**, *7*, 146–157. [CrossRef], [Google Scholar], [Publisher]

[20] A. Daina, O. Michielin, V. Zoete, *Sci. Rep.*, **2017**, *7*, 42717. [CrossRef], [Google Scholar], [Publisher]

[21] Z. Li, H. Wan, Y. Shi, P. Ouyang, *J. Chem. Inf. Comput. Sci.,* **2004**, *44*, 1886–1890. [CrossRef], [Google Scholar], [Publisher]

[22] W.J. Hehre, W.W. Huang, Chemistry with computation: an introduction to SPARTAN. Wavefunction, Inc, Irvine, **1995**. [Google Scholar]

[23] A. Mirzaie, *J. Med. Chem. Sci.,* **2018**, *1*, 31–32. [CrossRef], [Google Scholar], [Publisher]

[24] Y. Yao, T. Huo, Y.L. Lin, S. Nie, F. Wu, Y. Hua, J. Wu, A.R. Kneubehl, M.B. Vogt, R. Rico-Hesse, Y. Song, *J. Am. Chem. Soc.*, **2019**, *141*, 6832-6836. [CrossRef], [Google Scholar], [Publisher]

[25] O. Trott, A.J. Olson, *J. Comput. Chem.*, **2010**, *31*, 455-461. [CrossRef], [Google Scholar], [Publisher]

[26] M. Sravani, A. Kumaran, A.T. Dhamdhere, N.S. Kumar, *Int. J. Res. Appl. Sci. Biotechnol.*, **2021**, *8*, 154-161. [CrossRef], [Google Scholar], [Publisher]

[27] D.E. Pires, T.L. Blundell, D.B. Ascher, *J. Med. Chem.*, **2015**, *58*, 4066-4072. [CrossRef], [Google Scholar], [Publisher]

[28] D.E. Arthur, A.N. Samuel, S. Ejeh, S.E. Adeniji, O. Adedirin, M. Abdullahi, *Sci. Afr.*, **2020**, *10*, e00612. [CrossRef], [Google Scholar], [Publisher]

[29] S.N. Adawara, G.A. Shallangwa, P.A. Mamza, A. Ibrahim, *Sci. Afr.*, **2021**, *13*, e00907. [CrossRef], [Google Scholar], [Publisher]

[30] C.A. Lipinski, *Advanced drug delivery reviews*, **2016**, *101*, 34–41. [CrossRef], [Google Scholar], [Publisher]

[31] P. Ertl, A. Schuffenhauer, *J. Cheminformatics*, **2009**, *1*, 1–1. [Google Scholar]

[32] J.B. Baell, G.A. Holloway, *J. Med. Chem.*, **2010**, *53*, 2719–2740. [CrossRef], [Google Scholar], [Publisher]

[33] S.S. Mishra, C.S. Sharma, H.P. Singh, H. Pandiya, N. Kumar, *Int. J. Pharmaceut. Phytopharmacol. Res.*, **2016**, *6*, 77–79. [Google Scholar]

[34] P.F. Hollenberg, *Drug metabolism reviews*. **2002**, *34*, 17–35. [CrossRef], [Google Scholar], [Publisher]

[35] A. Serretti, R. Calati, I. Massat, S. Linotte, S. Kasper, Y. Lecrubier, R. Sens-Espel, J. Bollen, J. Zohar, J. Berlo, P. Lienard, *Int. clin. psychopharmacol.*, **2009**, *24*, 250–256. [CrossRef], [Google Scholar], [Publisher]